

## **Transmission electron microscopy of silicon-Pyrex electrostatic bonds.**

**A T J van Helvoort, K M Knowles, C B Boothroyd and J A Fernie\***

Department of Materials Science and Metallurgy, University of Cambridge, Pembroke Street, CB2 3QZ, Cambridge, U.K.

\*Advanced Materials and Processes, TWI, Cambridge, CB1 6AL, U.K.

**ABSTRACT:** Electrostatic bonding is an important technique in the production of certain silicon devices. Despite this, the actual bonding mechanism is not well understood. Here TEM with EDX is used to characterise Si-Pyrex electrostatic bonds. Bright field TEM and EDX clearly show the formation of a cation-depleted region in the Pyrex adjacent to an electrostatic bond and can monitor the width of this region as a function of process conditions. To date, evidence has not been found for a discrete silica layer widely assumed to form at the interface during bonding.

### **1. INTRODUCTION**

Electrostatic bonding, also known as anodic or field-assisted bonding, is a simple, fast and reliable technique to produce strong bonds between an ionic conducting glass and a semiconductor or a metal. For instance, this bonding technique is used to make Si/Pyrex pressure sensors.

Intriguingly, the bonding mechanism is not completely understood. The movement of cations in the Pyrex in an electric field, which is essential for creating the bonding force, can be monitored by a number of techniques (see, for example, Lepienski et al. (1993)). In addition, it is widely believed that a discrete silica reaction layer  $\sim 10$  nm thick is formed at the depleted Pyrex-silicon interface and is responsible for the permanent strong bond (Wallis and Pomerantz, 1969). However, direct proof for such a layer is lacking – the experiments which have shown evidence for such a layer do not have unambiguous interpretations.

In this paper we report for the first time TEM results from a number of Si-Pyrex electrostatic bonds. These results show clear evidence for the cation-depleted regions in the Pyrex, but do not reveal a separate silica layer at the depleted Pyrex-silicon interface.

### **2. EXPERIMENTAL**

Squares of 0.3 mm thick n-Si (001) ( $R_a = 0.01 \mu\text{m}$ ) and 3 mm thick Pyrex ( $R_a = 0.02 \mu\text{m}$ ), both with 1 cm sides, were bonded between two heated plate electrodes under a vacuum of  $5.5 \times 10^{-5}$  mbar and an initial load of 200 N. Bonding was studied for times of 10 – 1800 s, voltages of 250 – 1500 V and temperatures in the range 300 – 500 °C.

For TEM, cross-sections of the bonds were sliced, ground and polished to 50  $\mu\text{m}$  thickness and dimpled at the interface. A copper support ring was attached before argon-ion milling. The samples did not require a further conductive coating to study the interfacial region in the TEM.

Layer thicknesses were measured on negatives taken on a 200 kV JEOL 200CX TEM. Dark field series, through focus series and energy dispersive X-ray analysis (EDX) were undertaken on a 300 kV Philips CM30 TEM.

### 3. RESULTS AND DISCUSSION

Bright field TEM images of three electrostatic bonds are shown in Figs. 1(a) – (c). At each bond a bright layer, C, 0.5 – 1.7  $\mu\text{m}$  thick is visible in the Pyrex, adjacent to the Pyrex–silicon interface. A black line, D, is present in layer C, situated  $\sim 0.2 \mu\text{m}$  from the edge of the layer with the bulk Pyrex. EDX analyses (Fig. 2) show that C is a sodium depletion layer and D is a pile-up of potassium. These observations agree with results on the movement of sodium and potassium during electrostatic bonding inferred from other techniques such as ion-scattering spectrometry (Carlson et al. 1974). Dark field images show the same features, but less clearly.

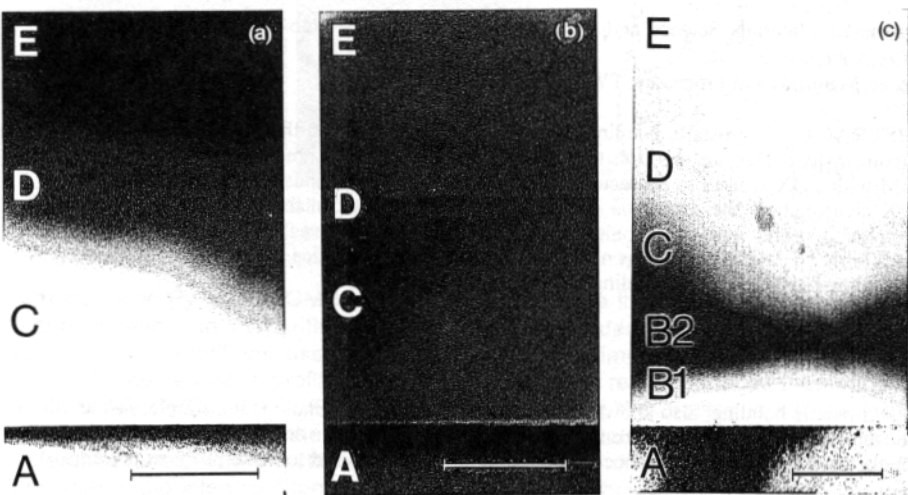


Fig. 1: TEM bright field images of electrostatic bonds formed at: (a) 350 °C, 1000 V and 60 s, (b) 350 °C, 1000 V and 60 s, followed by 350 °C, – 1000 V and 60 s, and (c) 350 °C, 1000 V and 600 s. A is silicon and E is Pyrex. In each micrograph the scale bar is 500 nm.

During conventional electrostatic bonding of silicon to Pyrex, the silicon is the anode and the Pyrex is the cathode. The mobile cations in Pyrex move towards the cathode during the bonding process and a cation-depleted layer is formed. The less mobile cations (potassium) pile up under the depletion edge of the more mobile cations (sodium). The size of the sodium depletion layer and the position of the centre of the pile-up of potassium ions both depend on the principal process parameters of time, voltage and temperature, as shown in Fig. 3. The sodium depletion size,  $d$ , can be estimated from the amount of charge transported during the bonding process (Carlson et al 1972):  $d = \int I dt / A \rho e$ , where  $I$  (in A) is the current measured at time  $t$  (in s).  $A$  is the area of the interface,  $\rho$  is the sodium ion density in the Pyrex ( $5.8 \times 10^{17}$  ions/ $\text{mm}^3$ ) and  $e$  is the electronic charge.

The overall trends in the sodium depletion layer sizes shown in Fig. 3 measured from a number of TEM micrographs are consistent with the trends for the sodium depletion layer sizes estimated from  $d = \int I dt / A \rho e$  for bonding times of less than 60 s. However, the formula for  $d$  overestimates the observed layer sizes by a factor of more than three. In addition, measured

depletion layer thicknesses for bonding times longer than 600 s plateau at thicknesses in the range 1.6 – 1.7  $\mu\text{m}$ , in contrast to the observation that a residual current is still recorded during electrostatic bonding for these long times. An explanation for these differences between experimental observation and theoretical prediction is that in applying the above formula it is assumed that the current is due to the transport of sodium ions alone. It has been suggested in the literature that after the sodium depletion layer is fully formed, the residual current is due either to the movement of non-bridging oxygen ions (NBOs) (Carlson et al 1972) or electrons (Krieger and Lanford 1988).

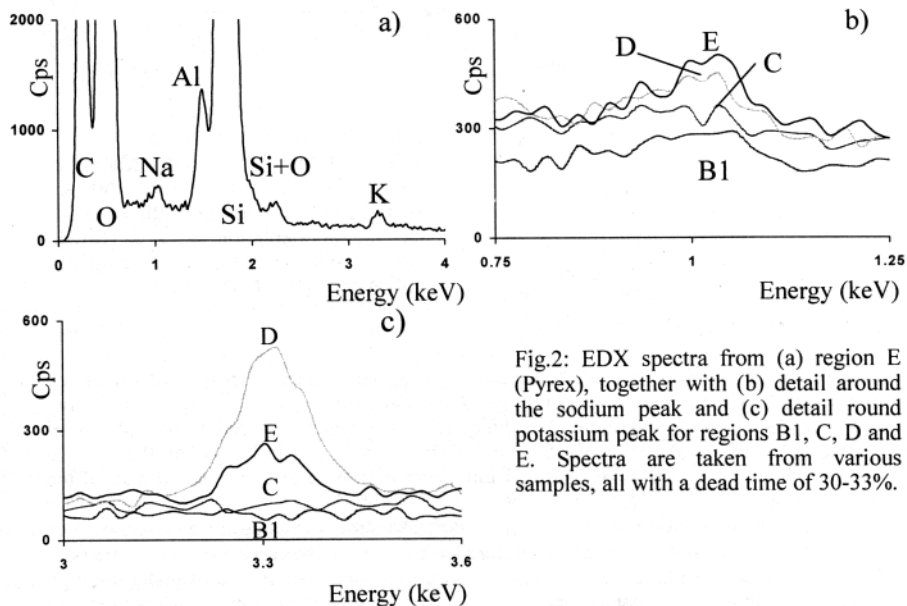


Fig.2: EDX spectra from (a) region E (Pyrex), together with (b) detail around the sodium peak and (c) detail around potassium peak for regions B1, C, D and E. Spectra are taken from various samples, all with a dead time of 30-33%.

The bright field image in Fig. 1(b) is from a sample where a reverse bias has been applied directly after conventional bonding, so that the Pyrex becomes the anode. The silicon and Pyrex remain bonded. It is apparent from Fig. 1(b) that the layer structure can still be seen and that it has the same dimensions as in Fig. 1(a). This suggests that an irreversible structural change occurs in the glass during conventional electrostatic bonding. This permanent structural change is most probably the reason for the high level of contrast between the Pyrex and the sodium-depleted Pyrex.

For bonding times of  $\geq 600$  s at temperatures above 400  $^{\circ}\text{C}$  a second brighter layer 0.1 – 0.7  $\mu\text{m}$  thick appears at the depleted Pyrex-silicon interface, such as the layer labelled B1 in Fig. 1(c). The width of this layer is less uniform than the sodium depletion layer and the potassium pile-up line. The edge of this layer is often accompanied by a darker 'shadow', such as B2 in Fig. 1(c). In comparison with the rest of the sodium depletion layer, C, the EDX counting rate is lower for B1 and higher for B2. The EDX spectra from B1, B2 and C are identical within the limits of the resolution of the EDX detector used. Therefore, the contrast differences between B1, B2 and C are due to thickness variations parallel to the electron beam.

The origin of B1 is unclear. Possible reasons are (i) an ion-milling artefact, (ii) a region where non-bridging oxygen ions have been transported towards the silicon-depleted Pyrex interface as suggested by Carlson et al (1974), or (iii) a structural change within the glass such as densification or network polymerisation during bonding which influences the thinning rate during ion milling. EDX spectra from B1 clearly show Al peaks and EELS spectra from B1 indicate that it contains both Al and B, suggesting that B1 is not an anodic silica layer formed during bonding.

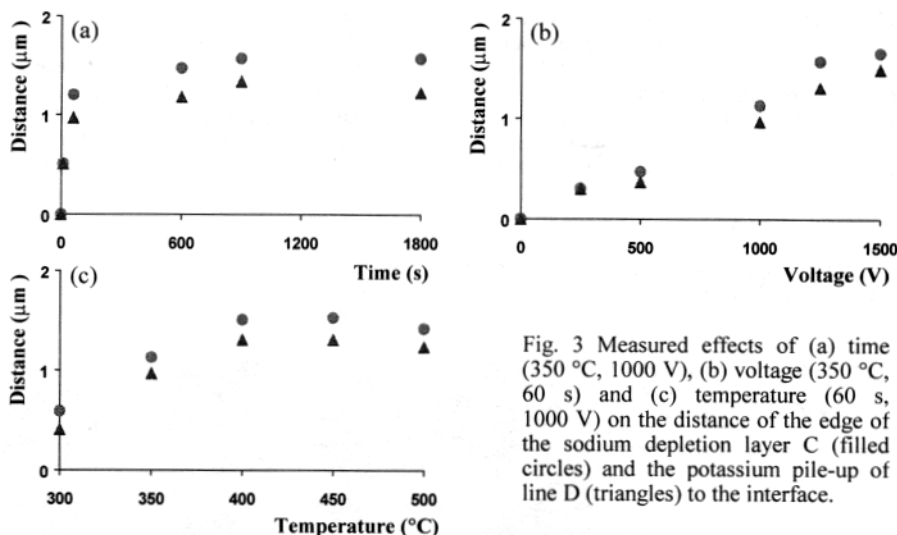


Fig. 3 Measured effects of (a) time (350  $^{\circ}\text{C}$ , 1000 V), (b) voltage (350  $^{\circ}\text{C}$ , 60 s) and (c) temperature (60 s, 1000 V) on the distance of the edge of the sodium depletion layer C (filled circles) and the potassium pile-up of line D (triangles) to the interface.

Estimates of the width of any silica reaction layer at the depleted Pyrex-silicon interface range from 1.4 nm (Albaugh et al 1992) through 7 nm (Veenstra et al 2001) up to 10–20 nm (Baumann et al 1995), all using indirect techniques. The oxygen required is thought to be transported towards the depleted Pyrex-silicon interface under the influence of the applied electric field in the form of NBOs or hydroxyl ions from dissolved water in the surface of the glass (Veenstra et al 2001).

To date, our experimental observations have failed to show evidence for a separate silica layer at the depleted Pyrex-silicon interface. Before we can support the proposition that the final bond is formed by anodic oxidation, and not for instance by surface modifications under the high electrostatic force, more experimental work is needed. In principle, the boron K edge is useful to monitor the small difference (4.5–5 at.% of B) between silica and the depleted glass by EELS, but we have experienced charging problems in STEM experiments which so far have prevented us from obtaining a good enough spatial resolution.

## ACKNOWLEDGEMENTS

We would like to thank the UK Department of Trade & Industry for funding the project through the Postgraduate Training Partnership scheme between the University of Cambridge and TWL.

## REFERENCES

- Albaugh K B and Rasmussen D H 1992 *J. Am. Ceram. Soc.* **75**, 2644  
 Baumann H, Mack S and Münzel H 1995 *The Electrochem. Soc. Proc. Series* **95-7**, pp 471-8  
 Carlson D E, Hang K W and Stockdale G F 1972 *J. Am. Ceram. Soc.* **55**, 337  
 Carlson D E, Hang K W and Stockdale G F 1974 *J. Am. Ceram. Soc.* **57**, 295  
 Krieger U K and Lanford W A 1988 *J. Non-Crystalline Solids* **102**, 50  
 Lepienski C M, Giacometti J A, Leal Ferreira G L, Freire, F L and Achete C A 1993 *J. Non-Crystalline Solids* **159**, 204  
 Veenstra T T, Berenschot J W, Gardeniers J G E, Sanders R G P, Elwenspoek M C and van den Berg A 2001 *J. Electrochem. Soc.* **148**, G68  
 Wallis G and Pomerantz D I 1969 *J. Appl. Phys.* **40**, 3946